Available online at www.sciencedirect.com
SCIENCE DIRECT®
Journal of Chromatography A, 1018 (2003) 155–167
JOURNAL OF CHROMATOGRAPHY A
www.elsevier.com/locate/chroma

Investigation of particle-based and monolithic columns for cation exchange protein displacement chromatography using poly(diallyl-dimethylammonium chloride) as displacer

Beata Schmidt, Christine Wandrey, Ruth Freitag*

Laboratory of Chemical Biotechnology, Institute of Chemical and Biological Process Sciences, Faculty of Basic Sciences, Swiss Federal Institute of Technology Lausanne, Ecublens, Lausanne CH-1015, Switzerland

Received 3 March 2003; received in revised form 21 July 2003; accepted 22 July 2003

Abstract

The overall topic of the investigation was the separation of basic proteins by cation exchange displacement chromatography. For this purpose two principal column morphologies were compared for the separation of ribonuclease A and α-chymotrypsinogen, two proteins found in the bovine pancreas. These were a column packed with porous particles (Macro-Prep S, 10 μm, 1000 Å) and a monolithic column (UNO™ S1). Both columns are strong cation exchangers, carrying $-SO_3^-$-groups linked to a hydrophilic polymer support. Poly(diallyl-dimethylammonium chloride) (PDADMAC), a linear cationic polyelectrolyte composed of 100–200 quaternary pyrrolidinium rings, was used as displacer. The steric mass action (SMA) model and, in particular, the operating regime and dynamic affinity plots were used to aid method development. To date the SMA model has been applied primarily to simulate non-linear displacement chromatography of proteins using low molar mass displacers. Here, the model is applied to polyelectrolytes with a molar mass below 20 000 g mol^{-1}, which corresponds to a degree of polymerization below 125 and an average contour length of less than 60 nm. The columns were characterized in terms of the adsorption isotherms (affinity, capacity) of the investigated proteins and the displacer.
© 2003 Elsevier B.V. All rights reserved.

Keywords: Displacement chromatography; Steric mass action model; Stationary phases, LC; Monolithic columns; Poly(diallyl-dimethylammonium chloride); Proteins

1. Introduction

Displacement chromatography has been suggested as a powerful mode for preparative biochromatography, which may have significant advantage over the currently preferred (overloaded) elution mode [1]. In ion exchange displacement chromatography, the column is initially equilibrated with a relatively low ionic strength carrier buffer, assuring strong binding. The feed mixture is then loaded onto the stationary phase followed by the so-called displacer. The displacer has a higher stationary phase affinity than the molecules of interest. Hence, as the displacer front advances, the number of available stationary phase binding sites is

Abbreviations: GPC, gel permeation chromatography; PDADMAC, poly(diallyl-dimethylammonium chloride); RPC, reversed-phase liquid chromatography; SMA, steric mass action

* Corresponding author. Tel.: +41-21-693-6108; fax: +41-21-693-6030.
E-mail address: ruth.freitag@epfl.ch (R. Freitag).

0021-9673/$ – see front matter © 2003 Elsevier B.V. All rights reserved.
doi:10.1016/S0021-9673(03)01326-8

steadily reduced. At this stage the more strongly bound substances begin to displace the less well bound ones from the stationary phase surface and, as a result, the feed mixture is resolved into consecutive zones of the pure substances, the so-called "displacement train". If desired, the substances' concentration can concomitantly be increased by a suitably choice of the displacer concentration. After the breakthrough of the displacer front, the column is regenerated and re-equilibrated.

The displacer is of obvious importance in displacement chromatography. This—preferably non-toxic—substance should have a sufficiently high affinity to the stationary phase to displace the components, but still allow easy removal from the matrix in the column regeneration step. A variety of substances have been proposed for this purpose, including charged molecules [2], dendritic oligomers [3], antibiotics [4] and even proteins [5]. Especially for ion exchange chromatography, various polyelectrolytes have been suggested as efficient protein displacers [6,7].

The design and application of polyelectrolytic displacers requires good knowledge of the interaction between the charged molecules and the oppositely charged stationary phase surface. An overview of the current polyelectrolyte adsorption theory and models can be found in Fleer et al. [8]. In addition to the predominant interaction mode—electrostatic in the case of ion exchange phases—a variety of secondary interactions may influence the displacer binding. A recent investigation by Shukla [9] has demonstrated how the affinities of homologous low molar mass displacers (molar mass $<1000\,\mathrm{g\,mol^{-1}}$) may vary for different ion exchange phases due to such secondary interactions.

In addition to the stationary phase surface chemistry, the morphology may also be of influence. Most chromatographic separations of biomolecules are carried out on columns packed with porous particles. Especially for displacement chromatography, these materials have some drawbacks. While the porous structure assures the desired large surface per volume area, the separation speed (mobile phase flow rate) is limited, else mass transfer limitations commence to have a negative influence on the column performance. On the other hand, it has been shown that the use of continuous-bed (monolithic) columns may have considerable advantages in displacement chromatography [10,11]. In monolithic columns, the stationary phase consists of a porous polymer rod. Due to this morphology (flow through pores) and a somewhat lower backpressure, such columns allow the use of much higher flow rates than the conventional ones without loss in resolution and efficiency. The group of Natarajan and Cramer [12] has recently presented an iterative optimization routine for different types of separation and different particle sizes of resin. They have shown that under certain conditions, a relatively large particle size material (34 μm) can perform better than a smaller one (8 μm). However, this was primarily due to a significantly higher capacity of the larger diameter material. Other authors have therefore also reported opposite findings [13].

In the present paper, two column morphologies—packed particles and continuous-bed—are compared concerning their performance in cation exchange displacement chromatography of ribonuclease A and α-chymotrypsinogen (two basic proteins from bovine pancreas) using a novel type of poly(diallyldimethylammonium chloride) (PDADMAC) as displacer [14,15]. This displacer is highly hydrophilic and carries one permanently charged quaternary ammonium group in each monomeric unit. In addition, this particular PDADMAC is characterized by a relatively narrow distribution of the (adjustable) molar mass. As a consequence, a given PDADMAC preparation has a defined and uniform affinity to the stationary phase.

2. Materials and methods

2.1. Materials

Sodium phosphate, sodium chloride, ammonium sulfate, proteins and chemicals for buffer and eluent preparation were purchased from Sigma (Buchs, Switzerland). Water was purified using an Elix-3 system (Millipore, Bedford, MA, USA). Raw solutions of PDADMAC were prepared by ACIMA, Rohm & Haas (Buchs, Switzerland) following a synthesis protocol published previously [16]. The subsequent polymer purification, preparation and freeze-drying were also described therein.

The strong cation exchanger columns were both from BioRad (Hercules, CA, USA). The particle-based column was a BioScale S2 filled with 10 μm Macro-Prep S particles (nominal pore size

1000 Å). The beads consist of a highly hydrophilic methacrylate-based support, to which strong cation exchanger groups ($-SO_3^-$) are linked. The monolithic column was a UNO^{TM} S1. UNO-columns are produced by an in situ polymerization of monomers and ionomers; the exact composition is proprietary. The result is a column consisting of a single highly porous polymer rod. Again, $-SO_3^-$-groups are linked to the support to provide the cation exchange capability.

For the analysis of the displacement fractions by reversed-phase liquid chromatography (RPC), an Agilent ZORBAX 300SB-C_{18} column (4.6 mm × 150 mm, 5 μm particles) from Agilent Technologies, USA was used.

2.2. Experimental methods

The purity, the molar mass and the molar mass distribution of the polymers were ascertained by gel permeation chromatography (GPC) as described previously [16].

The number of theoretical plates, N, used to construct the van Deemter curve were calculated from the retention volume V_r (taken as the peak maximum) and the peak width at half-height, $W_{0.5}$, of an inert tracer, as follows:

$$N = 5.54\left(\frac{V_r}{W_{0.5}}\right)^2 \quad (1)$$

van Deemter curves were constructed in the flow rate range of 0.1–2.2 ml min^{-1} using a system assembled from a model 422 HPLC pump (Bio-Tek Kontron Instruments, Basel, Switzerland), a Valco 10-port valve (Valco, Houston, TX, USA), and a Spectroflow 757 UV-detector (Kratos Analytical, Ramsey, NJ). The mobile phase was a 75 mM sodium phosphate buffer pH 7.2. Acetone (2%, v/v) was used as inert tracer.

The ion capacities of the stationary phases, Λ, were determined as follows: The columns were first equilibrated with a 75 mM sodium (monobasic) phosphate buffer, pH 7.2, for approximately 10 column volumes, followed by a step gradient to a 1.0 M ammonium sulfate solution. The sodium content of the column effluent was analyzed by atomic absorption spectrometry (Perkin-Elmer, Model 1100A, Norwalk, CT, USA). For this the effluent fractions were diluted 1000 times in UHP water prior to measurements. Na^+ ion standards (10, 20, 50, 100 μM) were used for calibration.

Isotherms were obtained from measurements as suggested by Jacobson et al. [17]. For this, the chromatography system described in the previous paragraph was modified with two 5 ml preparative sample loops to introduce the various solutions. A flow rate of 0.5 ml min^{-1} was adjusted in this case.

The chromatographic system for the displacement experiments was identical to the one described for the van Deemter curve determination. The samples were injected by a 1 ml loop, whereas the displacer was introduced from a 5 ml preparative sample loop (Knauer, Berlin, Germany). A flow rate of 0.2 ml min^{-1} was used throughout. Two 75 mM sodium phosphate buffers were used as mobile phases, one with a pH of 7.2 the other with a pH of 5.0. Displacement separations were monitored by collecting fractions twice per minute (i.e. 100 μl each). Fractions were analyzed by reversed-phase HPLC, see below.

The analytical HPLC system for fraction analysis was assembled from a degasser (ERC-3112, Ercatech, Bern, Switzerland), a 422 pump and an HPLC gradient former 425 controlled by a Chromatography Station for Windows (all Bio-Tek Kontron Instruments, Basel, Switzerland). Detection (214 nm) was by a HPLC 535 UV detector (Bio-Tek Kontron Instruments, Basel, Switzerland). The fractions were diluted eight times in the same buffer, as used in the displacement separation of the proteins. Sample injection (20 μl) was by autosampler (HPLC 560, Bio-Tek Kontron Instruments, Basel, Switzerland). Buffer A was deionized water with 0.1% (v/v) trifluoroacetic acid added and buffer B acetonitrile with 0.1% (v/v) TFA added. The gradient was run from 10 to 90% B (10 min, 1.0 ml min^{-1}, 60 °C). Data collection and interpretation was carried out with the Kontron chromatography software. All substances of interest including the displacer were quantified by this method.

2.3. Determination of the SMA parameters

The steric mass action (SMA) model of non-linear chromatography was introduced by Brooks and Cramer in 1992 [18] and was used by us to aid method development. The calculation of the SMA

model parameters as well as of the dynamic affinity and the operating regime plots is essential for the understanding of the subsequent data handling and discussion. It will be shortly summarized herein.

According to the SMA model, the prediction of a displacement separation requires three parameters, the characteristic charge, ν, the steric factor, σ, and the adsorption equilibrium constant, K. All three have to be determined for both the displacer and the proteins [19]. The characteristic charge defines the number of interaction points between the surface and the molecule of interest, whereas the steric factor corresponds to the number of salt counter ions on the surface sterically hindered from the exchange with the mobile phase by the adsorbed target molecules. The adsorption equilibrium constant is a measure for the stationary phase affinity of the molecules.

The characteristic charge of the displacer, ν_D,

$$\nu_D = \frac{n}{n_D} = \frac{\Delta C_s}{C_D} \tag{2}$$

is calculated from n, the total amount of sodium ions displaced during a frontal chromatography experiment, and n_D, the amount of displacer molecules retained on the stationary phase. This ratio equals the ratio of ΔC_s, the step increase in the mobile phase counter-ion concentration, to C_D the displacer concentration.The steric factor of the displacer, σ_D, is calculated by Eq. (3):

$$\sigma_D = \left(\frac{\Lambda}{Q_D^{max}}\right) - \nu_D \tag{3}$$

where Λ is the ion capacity of the column and Q_D^{max} the maximum stationary phase capacity for the displacer. The equilibrium constant, K_D, of the displacer is calculated by Eq. (4):

$$K_D = \left(\frac{1}{\beta}\right) \Pi \left\{\frac{C_S}{\Lambda - (\nu_D + \sigma_D)(C_D/\beta)\Pi}\right\}^{\nu} \tag{4}$$

where β is the phase ratio of the column, Π is equal to $(V_B/V_0) - 1$, while C_S the initial salt concentration in the carrier. V_B and V_0 are the breakthrough volume of the substance and the dead volume of the column, respectively.

Isocratic linear elution experiments were carried out at various mobile phase salt concentrations to determine the characteristic charge, ν_P, and the equilibrium constant, K_P, of the proteins, according to Eq. (5):

$$\log k' = \log(\beta K_P \Lambda^{\nu_P}) - \nu_P \log C_S \tag{5}$$

where k' is the dimensionless retention time of the protein in question.

Eq. (5) allows the determination of both parameters by plotting $\log k'$ versus $\log C_S$. This plot yields a straight line with a slope of $-\nu_P$, and an intercept of $\log(\beta K_P \Lambda^{\nu_P})$.

The steric factor, σ_P, of the proteins was calculated from points in the non-linear range of the respective adsorption isotherms according to Eq. (6):

$$\sigma_P = \frac{\beta}{C_P \Pi}\left\{\Lambda - C_S\left[\frac{\Pi}{(\beta K_P)^{1/\nu_P}}\right]\right\} - \nu_P \tag{6}$$

2.4. Dynamic affinity and operating regime plots

The plot of $\log K$ as a function of ν with Δ (ratio of the stationary phase to the mobile phase concentration) as the axial intercept, the so-called “dynamic affinity plot”, can be used to illustrate and to predict the elution order in a displacement separation [20]. The dynamic affinity plot defines two regions, a region below the dynamic affinity line where all solutes have a lower dynamic affinity than the molecule of interest, and a region above the affinity line, where all solutes have a higher dynamic affinity and can therefore displace the molecule of interest. The slope of the plot is equal to $\log \lambda$, i.e. the logarithm of the dynamic affinity λ.

The operating regime plot defines boundaries between chromatographic modes [21]. These are the boundary between displacement and desorption (displacement line) and the boundary between displacement and elution (elution line). The first line of the operating regime plot is calculated by selecting values for C_D and substituting them into Eq. (8) in order to obtain the corresponding salt concentration C_{SC}:

$$C_{SC} = \left(\frac{K_D}{\Delta_D}\right)^{1/\nu_D} \Lambda - [(\nu_D + \sigma_D) C_D \Delta_D] \tag{7}$$

where Δ_D corresponds to the partition coefficient of the displacer (Q_D/C_D). The elution line is calculated by modifying values for the displacer’s partition coefficient and substituting these into Eqs. (8) and (9). The critical displacer concentration at which elution of the protein in the induced gradient occurs, is given by Eq. (8), while the corresponding critical salt

Table 1
Characteristic parameters of the BioScale S2 and the UNO^{TM} S1 columns

Parameter	BioScale S2	UNO^{TM} S1
Column dimensions*	5.2 cm × 0.7 cm	3.5 cm × 0.7 cm
Column volume, V_C	1.363 ml	0.918 ml
Column dead volume, V_0	0.671 ml	0.404 ml
Stationary phase volume, V_{st}	0.692 ml	0.513 ml
Support material*	Methacrylate	Proprietary
Interactive groups*	$-SO_3^-$	$-SO_3^-$
Particle/pore size*	10 μm/1000 Å	Monolith
Small ion capacity, Λ	367 mM	966 mM
Protein capacity$_{\alpha\text{-chymotrypsinogen}}$	2.4 mg ml^{-1} $_{\text{stationary phase}}$	0.9 mg ml^{-1} $_{\text{stationary phase}}$
Protein capacity$_{\text{ribonuclease A}}$	1.2 mg ml^{-1} $_{\text{stationary phase}}$	1.1 mg ml^{-1} $_{\text{stationary phase}}$
Phase ratio, β	1.032	1.27

Values indicated with the symbol (∗) were supplied by the manufacturer (BioRad), all other were measured by us.

concentration is given by Eq. (9).

$$C_D = \frac{\Lambda[1-(K_D/\Delta)^{1/\nu_D}(\Delta/K_P)^{1/\nu_P}]}{(\Delta/K_P)^{1/\nu_P}[\Lambda-((\nu_D+\sigma_D)\Delta)]} \quad (8)$$

$$C_{SC} = \left(\frac{K_D}{\Delta}\right)^{1/\nu_D} \Lambda - [(\nu_D+\sigma_D)C_D\Delta] \quad (9)$$

3. Results and discussion

3.1. Characterization of the particle-based and monolithic column

Two strong cation exchanger columns, a porous particle-based one (BioScale S2) and a monolithic one (UNO^{TM} S1) from the same manufacturer (BioRad) were investigated as supports in protein displacement chromatography. Table 1 comprises the characteristic parameters of the two column types.

With 0.92 ml, the total column volume of the monolithic column is almost 33% less than that of the particle-based one (1.36 ml). With 0.51 ml for the monolithic and 0.69 ml for the porous particle-based column, the difference in the stationary phase volume is less pronounced. This is due to the fact that the stationary phase of a monolithic column can fill the total column volume to a higher extent than it would be possible in the case of even a perfectly packed particle bed. In addition with 966 mM compared to 367 mM, the small ion capacity of the monolithic column is considerably higher than that of the particle-based one. While admittedly being rather high, similar if not higher values for the small ion capacity were measured for the UNO^{TM} column by other researchers before [10,12].

The van Deemter curves of the two columns were measured with acetone as well as with lysozyme (data not shown) as non-retained tracers (Fig. 1). As expected and observed previously [10,11], the particle-based column shows a dramatic decrease in plate number compared to the monolithic one at higher flow rate (>1 ml min^{-1}). However, in the flow rate region of interest here, namely 0.5 ml min^{-1} for the isotherm measurements and 0.2 ml min^{-1} for the displacement separations, little differences were seen in this parameter.

The two column types also show significant differences if the capacity for PDADMAC as a function of the average molar mass of the designated displacer molecule is compared (see Fig. 2).

The single component adsorption isotherms recorded for the smallest investigated PDADMAC, i.e. a compound with an average molar mass of 17 900 g mol^{-1} show an almost identical capacity of both column morphologies for this particular molecule. The PDADMAC with a molar mass of 32 400 g mol^{-1}, on the other hand, shows differences in both affinity and capacity as a function of the stationary phase type. In case of the particle-based column the capacity for the larger molecule decreases significantly (1 mg ml^{-1} of stationary phase as compared to 2.6 mg ml^{-1} in case of the monolithic column) suggesting an influence of the pore size, respectively, the accessible surface. Additionally, the initial slope of the respective PDADMAC adsorption isotherm

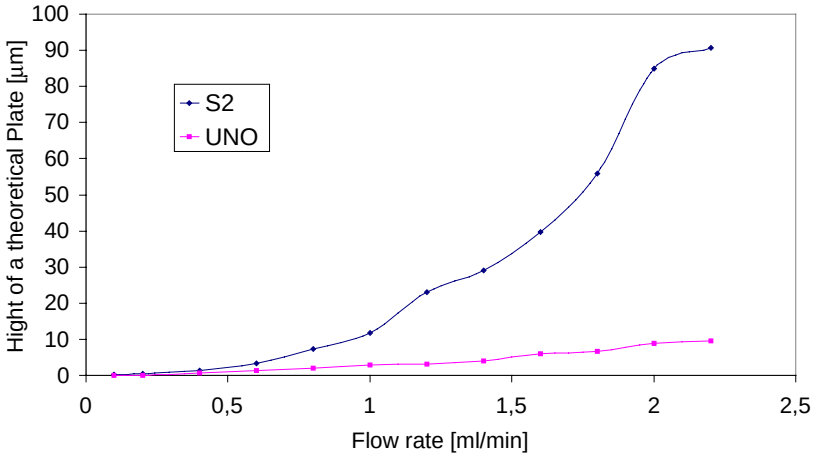

Fig. 1. van Deemter curves recorded for acetone (2% v/v) as non-retained tracer on the BioScale S2 and the UNO™ S1 column. Mobile phase: 75 mM phosphate buffer pH 7.2.

was much steeper (higher affinity) for the monolithic compared to the particle-based column. Presumably, in case of the porous material the larger displacer molecules are quickly excluded from the pores and hence from the major part of the adsorptive surface, while this effect is much less pronounced in case of the continuous monolithic column. The results are less conclusive in the case of the two proteins. Almost

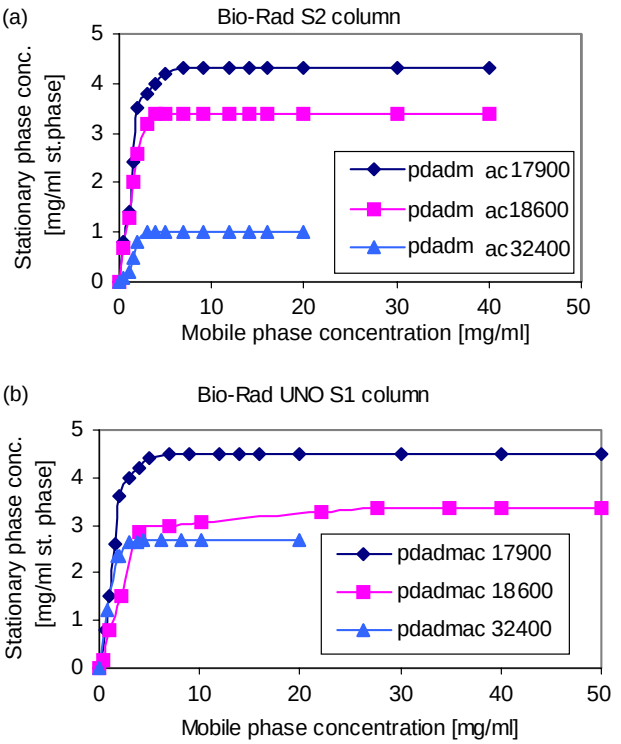

Fig. 2. Single component adsorption isotherms recorded for PDADMACs with molar masses of 16 500, 17 900, and 32 400 g mol^{-1}. Mobile phase: 75 mM phosphate buffer pH 7.2, flow rate: 0.5 ml min^{-1}. (a) BioRad S2 column, (b) UNO™ S1 column.

identical capacities are measured for the two column morphologies in case of ribonuclease A (molar mass 14 200 g mol^{-1}, isoelectric point 9.3), while the capacity for the larger α-chymotrypsinogen (molar mass 25 700 g mol^{-1}, isoelectric point 9.0) was in the same order of magnitude for the monolithic column, but considerably higher in case of the particle-based one.

From the results presented in Fig. 2, it is also clear that a general prediction from the polyelectrolyte adsorption theory [8], i.e. that under the chromatographic conditions selected here (low salt buffer concentration) the smaller PDADMAC molecules should bind more strongly to the stationary phases than the bigger ones, is indeed corroborated by the experimental results. This observation, previously made for the particle-based column morphologies [15,16], is observed without exception in case of the BioScale S2 column (particle-based stationary phase). It can thus be speculated that for this column the shorter PDADMAC molecules constitute more powerful displacers than the longer molecules of the same chemistry. In the case of the monolithic column (Fig. 2b) the general trend seems to be similar (vide isotherms of PDADMAC 17 900 and 18 600). However, the isotherm of PDADMAC 32 400 does not follow the trend. At present we are unable to explain this reproducibly observed experimental result.

3.2. Application of the SMA model

Displacement chromatography is known to be relatively sensitive to changes of the operating parameters. This is especially the case when small to medium size displacers are used. While this has advantages, e.g. the facile column regeneration by comparatively minor changes of the carrier composition, it also calls for a powerful method development strategy. The SMA model has been suggested as a means to improve and accelerate such method development [18]. The SMA model takes into account that the displacer will not only displace the feed compounds, but to some extent also the layer of adsorbed small counter ions, which is found on the stationary phase surface. This induces a salt step in front of the displacer zone, which in turn influences the micro-environment in the displacement train and hence in the end also the shape and the concentration of the various substance zones. To date the SMA model has been applied primarily to simulate non-linear displacement chromatography of proteins using low molar mass displacers. Here the model is applied to polyelectrolytes with a molar mass below 20 000 g mol^{-1}, which correspond to a degree of polymerization below 125 and an average contour length of less than 60 nm.

In order to apply the SMA model to the separation intended here, the SMA parameters, ν and σ, as well as the equilibrium constant K of the involved molecules had to be determined experimentally. More precisely, this study was performed including both column types, two different carrier pH (pH 5.0 and 7.2), the two proteins ribonuclease A (molar mass 14 200 g mol^{-1}, isoelectric point 9.3) and α-chymotrypsinogen (molar mass 25 700 g mol^{-1}, isoelectric point 9.0) as well as the designated displacer PDADMAC (molar mass 17 900 g mol^{-1}). A 75 mM phosphate buffer was chosen, since mobile phases with low ionic strength are commonly used in ion exchange chromatography when strong binding of charged compounds is intended. The resulting parameters are compiled in Table 2.

Table 2
SMA parameters (ν, σ, K) of proteins and displacer for the two columns measured at different carrier pH

	BioScale S2						UNO^{TM} S1					
	pH 5.0			pH 7.2			pH 5.0			pH 7.2		
	ν	σ	K	ν	σ	K	ν	σ	K	ν	σ	K
Ribonuclease A	2.1	80	7.17×10^{-1}	0.2	5.19	6.2×10^{-1}	7.21	129	1.52×10^{-5}	0.4	2.2	2.2×10^{-1}
α-Chymotrypsinogen	2.8	178	8.9×10^{-2}	3.9	25.7	3.9	3.44	463	3.17×10^{-3}	2.6	3.7	2.8×10^{-3}
Poly(DADMAC) 17 900	247	142	2.4×10^{32}	82	224	5.3×10^{16}	111	532	8.66×10^{2}	279	487	2.4×10^{-82}

The values for ribonuclease A and PDADMAC 17 900 g mol^{-1} at pH 7.2 have been published before in a different context, see [15] for details.

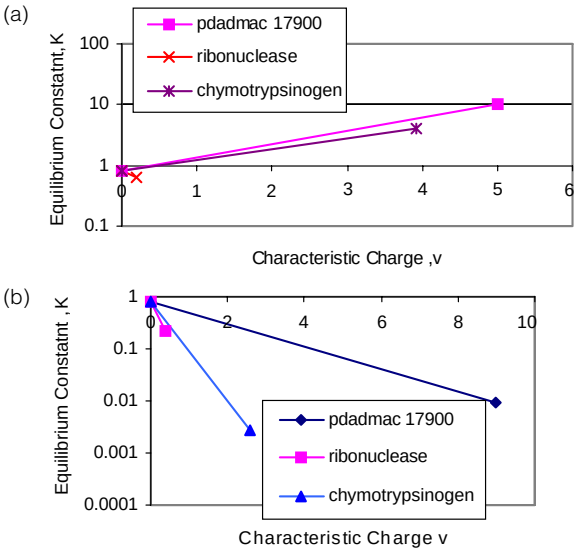

Fig. 3. Dynamic affinity plots for ribonuclease A, α-chymotrypsinogen and PDADMAC (molar mass 17 900 g mol^{-1}). Carrier: 75 mM phosphate buffer pH 7.2. (a) BioScale S2 column, (b) UNO^{TM} S1 column.

The determination of the SMA parameters according to the standard procedures described in Section 2, posed no problem in case of the proteins. Moreover, the values measured for both columns and pH values are comparable to those found in the pertinent literature for these or similar proteins (e.g. [22–24]). With the exception of α-chymotrypsinogen at pH 7.2, the characteristic charge for a given pH and protein is higher in the case of the monolithic column than the particle-based one. The values of the steric factor are consistently higher at the lower pH. In all cases, the equilibrium constant, K is much higher for the particle-based compared to the monolithic column.

In case of the displacer, the equilibrium constant was calculated from frontal experiments as suggested by Cramer [19]. However, the K-value thus determined is extremely high for the BioScale S2 column and appears to be unrealistically low in the case of the UNO^{TM} S1 column. At present no explanation can be given for these reproducibly obtained results. The values were nevertheless employed in a first attempt to find suitable conditions for a displacement separation of the two proteins. Fig. 3 shows the dynamic affinity plots constructed for the two columns using a 75 mM phosphate buffer pH 7.2 as carrier and PDADMAC molar mass 17 900 g mol^{-1} as displacer.

The Δ point of 0.8 in Fig. 3 corresponds to a PDADMAC concentration of 0.3 mM in the carrier. It was selected directly from the respective PDADMAC adsorption isotherm and corresponds to the ratio of the concentration of the displacer in the stationary to its concentration in the mobile phase (i.e. 0.3 mM). According to the dynamic affinity plots, PDADMAC 17 900 g mol^{-1} should indeed be able to displace ribonuclease A and α-chymotrypsinogen under the chosen conditions (namely a 75 mM phosphate buffer, pH 7.2) on both column types, since its dynamic affinity line is situated above the protein lines in all cases. In addition, the dynamic affinity plot indicates that the elution order in a putative displacement separation would be ribonuclease A, α-chymotrypsinogen and finally the displacer.

The operating regime plots (Fig. 4) were created to fine-tune the experimental conditions in regard to the salt concentration of the carrier and the displacer concentration.

In case of the particle-based column (Fig. 4a), the operating regime plot indicates that displacement separation of ribonuclease A and α-chymotrypsinogen should be possible with a displacer concentration between 0.22 and 0.82 mM (for ribonuclease A up to 1.6 mM) depending on the salt concentration of the mobile phase. The two parameters, i.e. the maximal displacer and the mobile phase salt concentration, are directly linked, since the upper limit of the displacer concentration for a given salt concentration is determined by the magnitude of the salt gradient induced under these conditions in front of the displacer step. If the salt step is too high, the proteins begin to elute in the induced salt gradient as opposed to being displaced by the displacer. In the case considered here, the upper limit of the carrier salt concentration appears to be 560 mM. When the displacer concentrations (range) recommended by the operating regime plot were used to create the corresponding affinity plots consistent results were obtained (data not shown).

For the monolithic column, the upper limit for the salt concentration is indicated by the operating regime plot as 450 mM (Fig. 4b). Protein separation should be possible with displacer concentrations ranging from 0.9 to 6.5 mM depending on the salt concentration of the carrier. This is a rather broad range of applicable

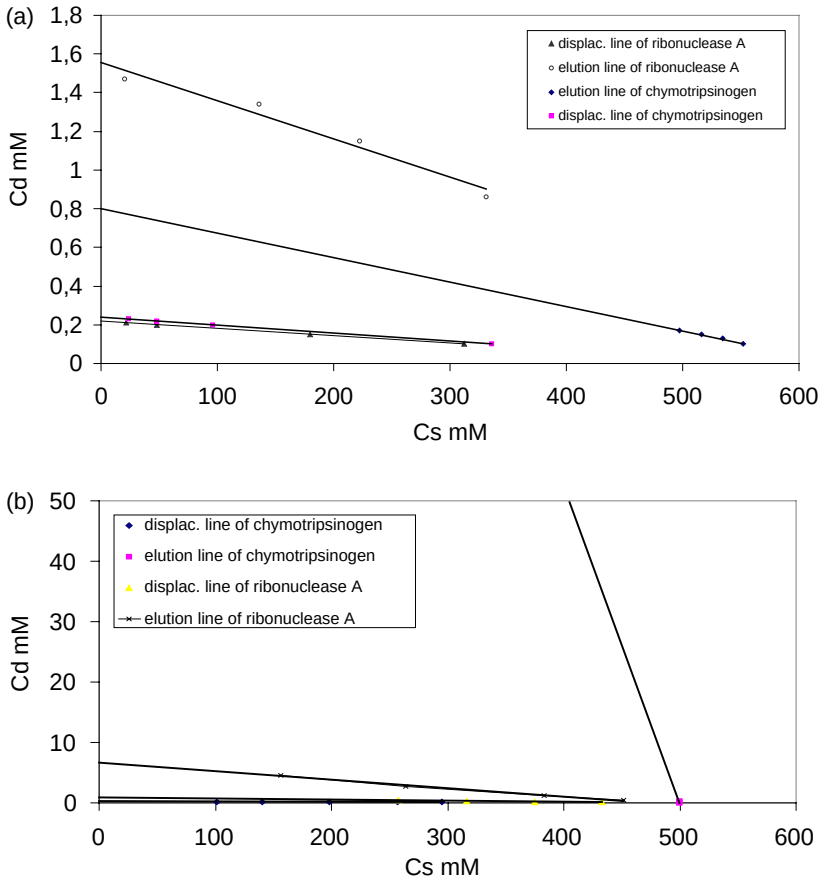

Fig. 4. Operating regime plots for the displacement separation of ribonuclease A and α-chymotrypsinogen using the indicated amount of PDADMAC (molar mass 17 900 g mol^{-1}) as displacer and a carrier (phosphate buffer pH 7.2) containing the indicated concentration of salt. (a) BioScale S2 column, (b) UNO^{TM} S1 column.

displacer concentrations compared to ranges usually calculated for conventional cation exchange materials, i.e. here also the BioScale column. Surprisingly, the previously chosen value of a displacer concentration of 0.3 mM is not included in this range. Moreover, when the extremes of the displacer concentration range were used to create the corresponding affinity plots, some unexpected results were obtained (Fig. 5 and Table 3).

For a displacer concentration of 0.9 mM (corresponding to a Δ point of 0.29, Fig. 5a), the elution order of the proteins should change, i.e. α-chymotrypsinogen, ribonuclease A rather than ribonuclease A, α-chymotrypsinogen, as predicted for the particle-based column, but also for the monolithic column at a displacer concentration of 0.3 mM.

Table 3
Slopes of the affinity line for ribonuclease A, α-chymotrypsinogen and PDADMAC (molar mass 17 900 g mol^{-1}) in a dynamic affinity plot constructed for different Δ points for the UNO^{TM} S1 column as stationary phase

	Δ		
	0.04	0.29	0.8
Mobile phase concentration (mM)	6.5	0.9	0.3
Poly(DADMAC) 17 900	−0.072	−0.296	−0.217
Ribonuclease A	1.853	−0.299	−1.400
α-Chymotrypsinogen	−0.444	−0.775	−0.945

A steeper slope indicates a higher stationary phase affinity of the corresponding substance.

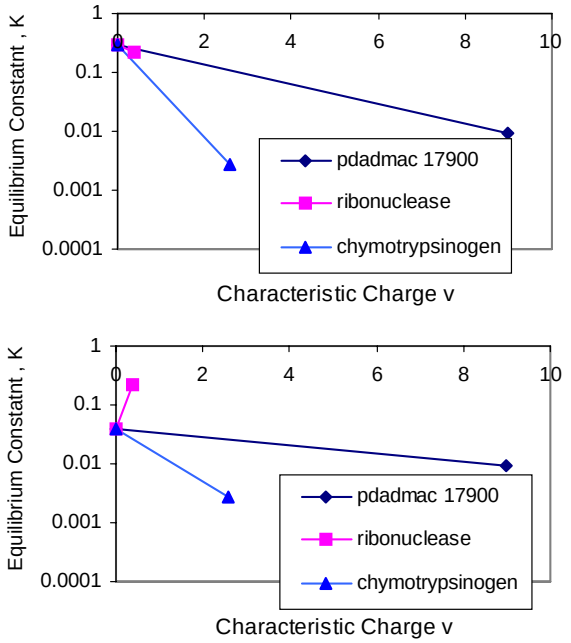

Fig. 5. Dynamic affinity plots for ribonuclease A, α-chymotrypsinogen and PDADMAC (molar mass 17 900 g mol^{-1}) at different displacer concentration. Carrier: 75 mM phosphate buffer pH 7.2, stationary phase: UNO^{TM} S1 column. (a) PDADMAC concentration 0.9 mM (Δ point 0.29), (b) PDADMAC concentration 6.5 mM (Δ point 0.04).

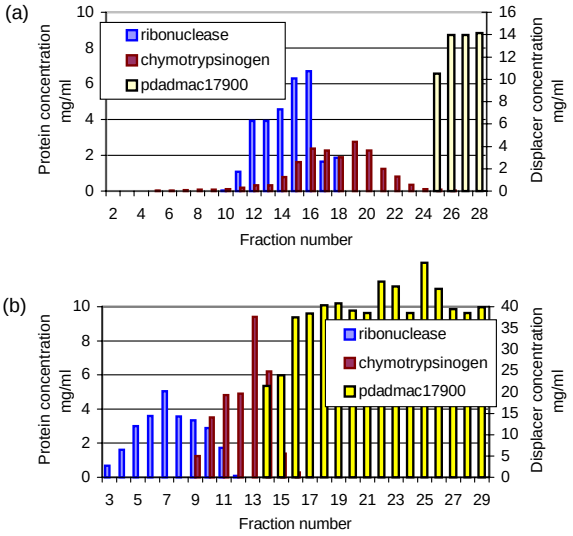

Fig. 6. Displacement separation of α-chymotrypsinogen and ribonuclease A using PDADMAC (molar mass 17 900 g mol^{-1}) as displacer. Stationary phase: BioScale S2 column, carrier: 75 mM phosphate buffer pH 7.2, flow rate: 0.2 ml min^{-1}. (a) Displacer concentration: 1.1 mM, α-chymotrypsinogen: 0.105 mM (2.7 mg ml^{-1}), ribonuclease A: 0.204 mM (2.9 mg ml^{-1}); (b) displacer concentration: 1.6 mM, α-chymotrypsinogen: 0.16 mM (4.1 mg ml^{-1}), ribonuclease A: 0.327 mM (4.6 mg ml^{-1}).

However, a displacement separation should in principle still be possible. For a displacer concentration of 6.5 mM (corresponding to a Δ point of 0.04, Fig. 5b) the PDADMAC should displace only the α-chymotrypsinogen but not the ribonuclease A, since its dynamic affinity line is below the dynamic affinity lines of the protein.

3.3. Displacement chromatography of proteins

The predictions of the SMA model were subsequently tested experimentally. The results are compiled in Fig. 6 for the particle-based column and in Fig. 7 for the monolithic one. The carrier was in both cases the initially chosen 75 mM sodium phosphate buffer (pH 7.2), as the suitability of this buffer had essentially been corroborated by the SMA model.

Two displacer concentrations (1.1 and 1.6 mM) were selected within the range suggested by the operating regime plots for the two columns, corresponding to concentrations of ca. 20 and 30 mg ml^{-1}. All displacement experiments were carried out in triplicate to assure the reproducibility of the results.

As predicted by the operating regime plot, the displacer concentration indeed has a significant influence on the separation of the protein mixture in the case of the particle-based column. In this case, the resolution was clearly improved when the displacer concentration was raised from 1.1 mM (Fig. 6a) to 1.6 mM (Fig. 6b). At a displacer concentration of 1.1 mM the two proteins were displaced by the PDADMAC, but they were not well separated. All earlier fractions contained a mixture of ribonuclease A and α-chymotrypsinogen. Fractions 18–24 contained pure α-chymotrypsinogen. The displacer front barely touched the α-chymotrypsinogen zone, which is also unusual in true displacement chromatography. It is unlikely that this is due to the induced salt step, since the effect is not observed at higher displacer concentration (Fig. 6b). The presence of an impurity in this zone cannot be completely ruled out, however, none was detected by either gel filtration chromatography

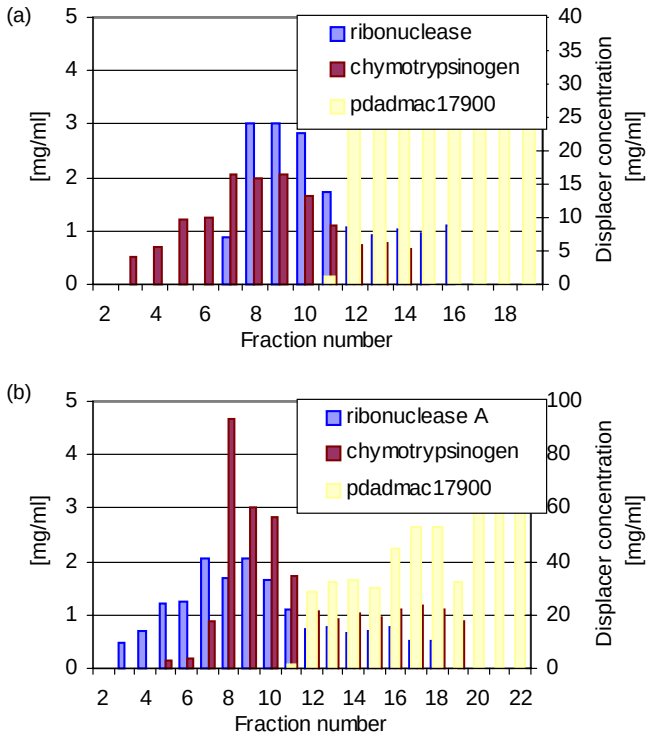

Fig. 7. Displacement separation of α-chymotrypsinogen and ribonuclease A using PDADMAC (molar mass 17 900 g mol^{-1}) as displacer. Stationary phase: UNO^{TM} S1 column, carrier: 75 mM phosphate buffer pH 7.2, flow rate: 0.2 ml min^{-1}. (a) Displacer concentration: 1.1 mM, α-chymotrypsinogen: 0.1 mM (2.5 mg ml^{-1}), ribonuclease A: 0.24 mM (3.3 mg ml^{-1}); (b) displacer concentration: 1.8 mM, α-chymotrypsinogen: 0.19 mM (4.8 mg ml^{-1}), ribonuclease A: 0.3 mM (4.2 mg ml^{-1}).

or mass spectrometry. At the higher displacer concentration (Fig. 6b), the displacement train was well developed and both proteins could be collected in pure form in some of the fractions. The elution order of the proteins was as predicted by dynamic affinity plot. The recovery yield for the ribonuclease A was 80% and for α-chymotrypsinogen 95%. Concomitantly, the chymotrypsinogen was concentrated by a factor of 2.

As it is obvious from Fig. 7, neither displacer concentration allowed the separation of the two proteins in the case of the monolithic column. This was somewhat surprising, since according to the operating regime plot both displacer concentrations should allow a displacement separation. On the other hand, the reversal of the elution order as a function of the displacer concentration, which was predicted by the affinity plots, is indeed observed. In the case of the lower displacer concentration the first four fractions contain pure α-chymotrypsinogen, while pure ribonuclease A is collected in the first fraction obtained in the experiment where the higher displacer concentration was chosen. An experimental verification of the prediction that even higher displacer concentrations would no longer allow the displacement of ribonuclease A was not possible, since such displacer solutions (6.5 mM = 116 mg ml^{-1}) are highly viscous and can no longer be pumped through the column.

The failure to obtain a good separation under the conditions suggested by the SMA model was even more surprising as it was possible to determine—by a purely trial-and-error-type of optimization—conditions, which did allow the separation of the two proteins by the monolithic column (Fig. 8).

PDADMAC with a molar mass of 16 500 g mol^{-1} instead of 17 900 g mol^{-1} was used as displacer in this case for reasons of availability. However, this was not responsible for the observed differences in the separation, data not shown. The improvement was rather

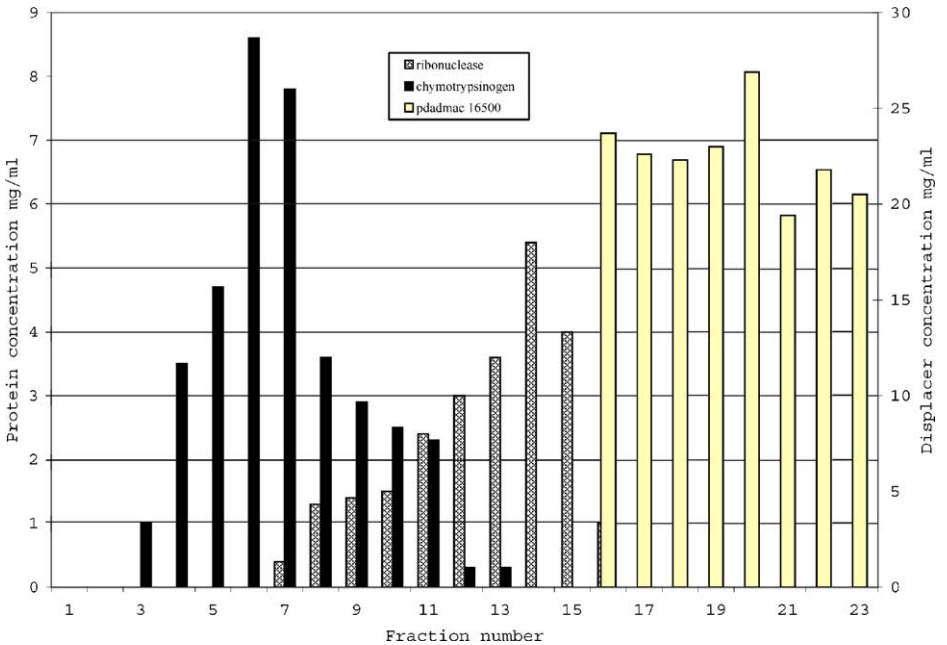

Fig. 8. Displacement separation of α-chymotrypsinogen A (2.75 mg) and ribonuclease A (2.5 mg) using PDADMAC (molar mass 16 500 g mol^{-1}) as displacer. Stationary phase: UNO^{TM} S1 column, mobile phase: 75 mM phosphate buffer pH 5.0, flow rate: 0.2 ml min^{-1}, displacer concentration: 1.2 mM.

due to the fact that in this experiment a 75 mM phosphate buffer with a pH 5.0 had been chosen as carrier. The feed mixture contained α-chymotrypsinogen and ribonuclease A at a concentration of 5 mg ml^{-1} each. The displacer concentration was 1.2 mM. Sixty percent of the ribonuclease A and 90% of the α-chymotrypsinogen were recovered under these circumstances.

4. Nomenclature

C_D	concentration of displacer in the mobile phase (mM)
C_P	concentration of a given protein in the mobile phase (mM)
C_S	initial salt concentration in the mobile phase (mM)
ΔC_s	step increase in the mobile phase counter-ion concentration (mM)
H	height of a theoretical plate
k'	dimensionless retention factor of a given protein
K_D	equilibrium constant of the displacer
K_P	equilibrium constant of a given protein
L	column length (cm)
n	total amount of sodium displaced by the displacer (mM)
n_D	displacer adsorbed on the stationary phase (mM)
N	plate number
Q_D	stationary phase concentration of the displacer (mM)
Q_D^{max}	maximum stationary phase capacity of the displacer (mM)
V_0	dead volume of the column (ml)
V_B	breakthrough volume of a given substance front (ml)
V_r	retention volume of a given species (ml)
$W_{0.5}$	peak width at half-height (cm)

Greek letters

β	column phase ratio
Δ	variable partition coefficient of the displacer
Δ_D	partition coefficient of the displacer
Λ	ion capacity of the column (mM)

ν_D characteristic charge of the displacer
ν_P characteristic charge of a given protein
σ_D steric factor of the displacer
σ_P steric factor of a given protein

Acknowledgements

This work is the result of a cooperation between the Laboratory of Polyelectrolytes and Biomacromolecules and the Laboratory of Chemical Biotechnology, Center of Biotechnology both Swiss Federal Institute of Technology Lausanne, Switzerland, as well as ACIMA Rohm & Haas, a producer of fine chemicals, also Switzerland. The research was supported by the Commission for Technology and Innovation, CTI (grant no: 3843.1). The help of Vesela Malinova with the adsorption isotherms is also most gratefully acknowledged.

References

[1] R. Freitag, in: G. Subramanian (Ed.), Bioseparation and Bioprocessing: Biochromatography, vol. 1, VCH Verlagsgruppe, Weinheim, 1998, p. 89.
[2] A.A. Shukla, S.S. Bae, J.A. Moore, K.A. Barnthouse, S.M. Cramer, Ind. Eng. Chem. Res. 37 (1998) 4090.
[3] G. Jayaraman, Y. Li, J.A. Moore, S.M. Cramer, J. Chromatogr. A 702 (1995) 143.
[4] A. Kundu, S. Vunnum, S.M. Cramer, J. Chromatogr. A 707 (1995) 57.
[5] R. Freitag, J. Breier, J. Chromatogr. A 691 (1995) 101.
[6] I.Y. Galaev, Biochemistry (Moscow) 63 (1998) 1258.
[7] Ch. Wandrey, R. Freitag, Polym. News 25 (2000) 54.
[8] G.J. Fleer, M.A.S. Cohen, J.M.H.M. Scheutjens, T. Cosgrove, B. Vincent, Polymers at Interfaces, Chapman & Hall, London, 1993.
[9] A.A. Shukla, K.A. Barnthouse, S.S. Bae, J.A. Moore, S.M. Cramer, J. Chromatogr. 814 (1998) 83.
[10] R. Freitag, S. Vogt, J. Biotechnol. 78 (2000) 69.
[11] S. Vogt, R. Freitag, Biotechnol. Prog. 14 (1998) 742.
[12] V. Natarajan, S.M. Cramer, J. Chromatogr. A 876 (2000) 63.
[13] S. Vogt, R. Freitag, J. Chromatogr. A 760 (1997) 125.
[14] R. Freitag, Ch. Wandrey, European Patent Appl. No: 98810231.5, International Patent Appl. No. PCT/IB 99/00455 (1998).
[15] B. Schmidt, Ch. Wandrey, R. Freitag, J. Chromatogr. A 944 (2002) 149.
[16] B. Schmidt, Ch. Wandrey, R. Freitag, H. Holzapfel, J. Chromatogr. A 865 (1999) 27.
[17] J. Jacobson, J. Frenz, Cs. Horváth, J. Chromatogr. 316 (1984) 53.
[18] C.A. Brooks, S.M. Cramer, AIChE J. 38 (12) (1992) 1969.
[19] S.D. Gadam, G. Jayaraman, S.M. Cramer, J. Chromatogr. 630 (1993) 37.
[20] S. Vunnum, S. Gallant, S. Cramer, Biotechnol. Prog. 12 (1996) 84.
[21] S.R. Gallant, S.M. Cramer, J. Chromatogr. A 771 (1997) 9.
[22] C.A. Brooks, S.M. Cramer, J. Chromatogr. A 693 (1995) 187.
[23] A. Kundu, S. Vunnum, G. Jayaraman, S.M. Cramer, Biotechnol. Bioeng. 48 (1995) 452.
[24] J. Gerstner, S.M. Cramer, Biotechnol. Prog. 8 (1992) 540.